Journal of the Serbian Chemical Society
JSCS-info@shd.org.rs • www.shd.org.rs/JSCS
J. Serb. Chem. Soc. 76 (12) 1661–1671 (2011)
JSCS–4238
UDC 546.46'72–31+665.652.7:54–32.004.12+54–36.004.12
Original scientific paper

Mg–Fe-mixed oxides derived from layered double hydroxides: a study of the surface properties

MILICA S. HADNAĐEV-KOSTIĆ[1*#], TATJANA J. VULIĆ[1#], RADMILA P. MARINKOVIĆ-NEDUČIN[1#], ALEKSANDAR D. NIKOLIĆ[2] and BRANISLAV JOVIĆ[2]

[1]*Faculty of Technology, University of Novi Sad, Bul. Cara Lazara 1, 21000 Novi Sad and* [2]*Faculty of Science, University of Novi Sad, Serbia*

(Received 29 April, revised 1 June 2011)

Abstract: The influence of surface properties on the selectivity of the synthesized catalysts was studied, considering that their selectivity towards particular hydrocarbons is crucial for their overall activity in the chosen Fischer–Tropsch reaction. Magnesium- and iron-containing layered double hydroxides (LDH), with the general formula: $[Mg_{1-x}Fe_x(OH)_2](CO_3)_{x/2}\cdot mH_2O$, $x = n(Fe)/(n(Mg)+n(Fe))$, synthesized with different Mg/Fe ratio and their thermally derived mixed oxides were investigated. Magnesium was chosen because of its basic properties, whereas iron was selected due to its well-known high Fischer-Tropsch activity, redox properties and the ability to form specific active sites in the layered LDH structure required for catalytic application. The thermally less stable multiphase system (synthesized outside the optimal single LDH phase range with additional Fe-phase), having a lower content of surface acid and base active sites, a lower surface area and smaller fraction of smaller mesopores, showed higher selectivity in the Fischer-Tropsch reaction. The results of this study imply that the metastability of derived multiphase oxides structure has a greater influence on the formation of specific catalyst surface sites than other investigated surface properties.

Keywords: Mg–Fe-LDHs; hydrotalcite; acid–base properties; Fischer–Tropsch reaction; selectivity.

INTRODUCTION

The Fischer–Tropsch (FT) reaction is an alternative route for converting syngas and entails the production of hydrocarbons in the presence of various metal-based catalysts. This reaction has been commercially used for many years and is still attracting much attention as a means of producing transportation fuels from coal, natural gas and biogas.[1–3] Iron-based catalysts are particularly used in the

* Corresponding author. E-mail: hadnadjev@tf.uns.ac.rs
# Serbian Chemical Society member.
doi: 10.2298/JSC110429149H

FT reaction due to their high activity and selectivity in syngas conversion with low H_2/CO ratios. Previous work on iron FT reaction catalyst focused on the improvement of the performances of Fe catalysts by various metal promoters.[3,4] This paper presents a study of the surface properties and catalytic performance of Mg–Fe-mixed oxides derived from layered double hydroxides (LDHs), synthesized within and outside the optimal range for attaining an LDH single phase. The possibility to vary the nature and content of M(II) and M(III) metals, the synthesis parameters and methods, enabling the design of LDH properties taking into consideration their future application, made these materials the subject of numerous investigations, especially in the field of environmental research. The LDH structure consists of positively charged layers compensated with anions positioned in the interlayers.[5] The layered structure collapses during thermal treatment leading to the formation of non-stoichiometric mixed oxides with a developed surface area, and specific acid–base and redox properties.[6] Mg–Fe-LDHs described by the formula $[Mg_{1-x}Fe_x(OH)_2](CO_3)_{x/2}\cdot mH_2O$, where x = Fe/[Mg+Fe] were studied. Magnesium was chosen as the M(II) ion because of its basic properties and the ability to enhance the selectivity towards FT products of iron catalysts.[4] In addition, according to the literature, mixed oxides obtained by thermal decomposition of LDHs can promote base-catalyzed reactions, particularly when the anions arranged in the interlayers are CO_3^{2-} anions, due to their important role in the basic properties of LDH structures.[7] Besides its well-known high FT activity, iron was selected as the active M(III) ion due to its redox properties and the ability to form specific active sites in the layered structure required for catalytic application.[8] The acid–base properties in correlation to other physico-chemical properties of the LDHs and their derived mixed oxides were examined. For the detection of the acid properties, pyridine adsorption was selected since, according to the literature,[9] pyridine molecules are excellent for the differentiation between Brønsted and Lewis acid sites on the surfaces of catalysts, as well as for ranking the strength and coordination of Lewis acid sites. The presence and nature of the base-active sites on the surface of the calcined samples were detected by phenol adsorption.

The focal point of this study was to investigate the influence of surface properties on the selectivity of the synthesized samples considering that their selectivity towards particular hydrocarbons is crucial for their overall activity in the FT reaction. The selectivity of the derived Mg–Fe-mixed oxides in the FT reaction was studied in correlation with different catalyst properties obtained by Mg––Fe-LDH synthesis within and outside the optimal range for a LDH single phase, especially with their textural properties, surface composition and morphology.

EXPERIMENTAL

Layered double hydroxides were synthesized by the low supersaturation coprecipitation method at a constant pH (9.6–9.9). Aqueous solution of $Mg(NO_3)_2\cdot 6H_2O$ and $Fe(NO_3)_3\cdot 9H_2O$

were continuously dropwise mixed (4 cm^3 min^{-1}) at a constant pH that was maintained by the simultaneous addition of Na_2CO_3 and NaOH solution.[10] The metal content was varied and two different values of x were chosen, one being $x = 0.3$, inside the optimal range for single LDH phase synthesis ($0.2 \leq x \geq 0.33$) and the other exceeding this range with $x = 0.7$. The samples were denoted according to their starting composition: sample 0.7Mg–0.3Fe ($x = 0.3$) and sample 0.3Mg–0.7Fe ($x = 0.7$). The LDHs were calcined at 500 °C for 5 h in air. Scanning electron microscopy (SEM) was used to analyze the morphology of the LDHs and derived mixed oxides and electron dispersive spectroscopy (EDS) for chemical analysis of the surface (JEOL, JSM-460 LV instrument). The acceleration voltage was 20 kV, with the working distance of 10 mm. Textural characterization of calcined samples (denoted K-), reduced samples (denoted H-) and samples after FT reaction (denoted TR-) was realized by low-temperature nitrogen sorption at –196 °C using Micromeritics ASAP 2010 instrument. The IUPAC classification of pores and the Barret, Joyner and Halend (BJH) method for the pore size distribution were used for the textural analyses. Thermal analysis, thermogravimetry (TG) and differential thermal analysis (DTA), of synthesized samples was performed using a Baehr STA503 instrument (BAEHR, Huellhorst, Germany) in the temperature range from room temperature to 1000 °C, at a heating rate of 5 °C min^{-1} under a static air atmosphere. The acid–base surface properties of the samples were investigated by detecting the amount of pyridine and phenol adsorbed on the surface of the samples using Fourier transform infrared (FTIR) analysis. The surface acidity of the samples was analyzed by the adsorption of pyridine on the sample surfaces. The calcined samples were degassed under a vacuum atmosphere (133.3 Pa) at room temperature for 30 min prior to the adsorption of pyridine. The pyridine was chemisorbed on the surface of the samples at room temperature under the vacuum atmosphere for 7 h. The surface base properties were analyzed by the adsorption of phenol on the sample surfaces. The same procedure was used for the adsorption, the only difference being the phenol chemisorption time was 24 h. The FTIR spectra of the previously adsorbed pyridine or phenol on the surface of the calcined samples were recorded in the range of 4000––400 cm^{-1} with a 2 cm^{-1} resolution on a Thermo Nicolet Nexus 670 FTIR spectrophotometer. Prior to the FTIR analysis, physically adsorbed pyridine or phenol was removed from the calcined samples under vacuum.[11] Selectivity tests were performed in a tubular quartz reactor in which the chosen catalysts were loaded. The entire reactor system was placed inside a temperature-regulated furnace. All the catalysts were *in situ* activated, prior to the FT investigation, at 350 °C for 2 h by the reduction treatment with pure hydrogen flow of 20 ml/min. After the reduction of the samples, the gas flow of reactants H_2 and CO having ratio of H_2:CO = 1:1 was adjusted and regulated by mass flow controllers. The FT reaction temperature was either 350 °C, 375 °C or 400°C. After passing through the reactor system, aliquots of the reaction mixture were taken with the syringe and analyzed. The reaction products were separated on a 30 m long PONA GC-capillary column and analyzed by gas chromatography using an HP 5890 Series II instrument equipped with thermal conductivity (TC) and flame ionization (FI) detectors. The selectivity (S) of catalysts was calculated using the following formula:

$$S = 100 \frac{F_x nC_x A_x}{\sum \left(F_{\text{product}} nC_{\text{product}} A_{\text{product}} \right)} \left[\% \right]$$

where S – selectivity, F – detector response factor, x – desired product, nC – number of C atoms in the product and A – value of the surface under the peak.

RESULTS AND DISCUSSION

Characteristic X-ray diffraction patterns for LDH were detected in both samples, LDH being the only crystalline phase in the $x = 0.3$ sample, whereas in the $x = 0.7$ sample, an additional goethite, FeO(OH), phase was also observed as published elsewhere.[10]

In order to determine the temperature leading to thermal decomposition of the LDHs, as well as to the formation and thermal stability of the mixed oxides, thermal analysis (TG-DTA) was performed. The mass loss and the corresponding endothermic/exothermic transitions of the synthesized Mg–Fe-LDH samples were simultaneously monitored. Two distinct transitions were observed on the TG–DTA curves of both samples (Fig. 1). The first endothermic transition in the temperature range from 90 to 200 °C accompanied by a mass loss is related to the dehydration of the samples, removal of the interlayer water and physically adsorbed water. The second endothermic transition, also accompanied by a mass loss, occurring in the temperature range from 300 to 400 °C, was assigned to dehydroxylation and decarbonation reactions. At higher temperatures (≈500 °C), broad endothermic peaks without mass loss were detected, probably due to spinel formation and Mg oxides. These findings are in good agreement with the literature.[12–14] Since in both samples the second endothermic transition was detected at temperatures lower than 500 °C, it was concluded that this temperature is sufficient for completion of the formation of mixed oxides and was selected as the calcination temperature. A comparison between the starting temperatures of spinel formation at ≈650 °C, corresponding to the beginning of the third endothermic peak in the sample 0.7Mg–0.3Fe, and at ≈550 °C for the sample 0.3Fe––0.7Mg suggests the formation of a mixed oxide phase in the single LDH phase sample 0.7Mg–0.3Fe which is more thermally stable at higher temperatures.

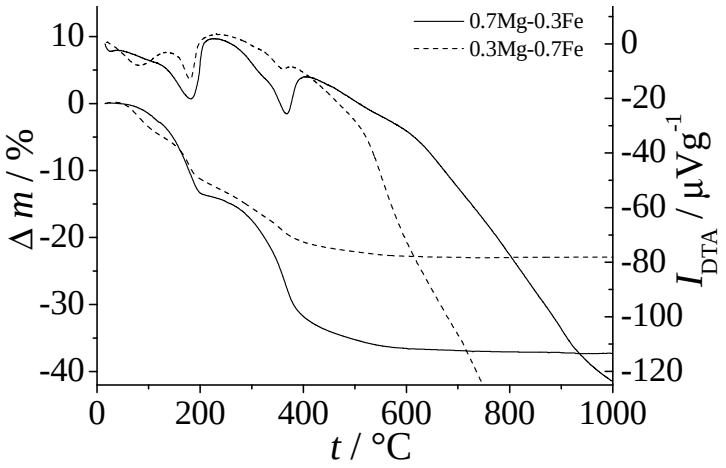

Fig. 1. TG–DTA Profiles of 0.7Mg–0.3Fe-LDH and 0.3Mg–0.7Fe-LDH.

For qualitative and quantitative analysis (EDS), Fig. 2, two locations for each synthesized sample (LDH-0.7Mg–0.3Fe and LDH-0.3Fe–0.7Mg) were used for the generation of EDS spectra. The provided elemental information revealed that the Mg and Fe contents on the surface of the samples are in good agreement with the targeted Mg/Fe ratios (sample 0.7Mg–0.3Fe: 70 mol % Mg and 30 mol % Fe, sample 0.3Mg–0.7Fe: 30 mol% Mg and 70 mol % Fe), confirming the successful synthesis of both samples. The pore size distributions of synthesized samples after calcination (K-0.7Mg–0.3Fe and K-0.3Mg–0.7Fe) and after the reduction treatment (H-0.7Mg–0.3Fe and H-0.3Mg–0.7Fe) are shown in Fig. 3. The multimodal pores size distribution of the K-0.7Mg–0.3Fe sample showed a small fraction of smaller mesopores ($d_p \approx 3$ nm) and a broad region with mesopores of 10 to 90 nm in diameter, having a maximum at 15 nm and a "shoulder" at 50 nm, indicating a significant fraction of mesopores. On the contrary, the K--0.3Mg–0.7Fe sample showed a region with mesopores from 20 to 70 nm having a maximum at 40 nm and smaller mesopores were not detected, Fig, 3a. These results are in good agreement with those of a previous study,[10] in which it was found that the presence of additional phases in a K-0.3Mg–0.7Fe sample negatively influenced the development of surface area (50 m^2 g^{-1} compared to 150 m^2 g^{-1} in a K-0.7Mg–0.3Fe sample), thereby disabling the formation of smaller mesopores and shifting the pore size distribution region to higher values.

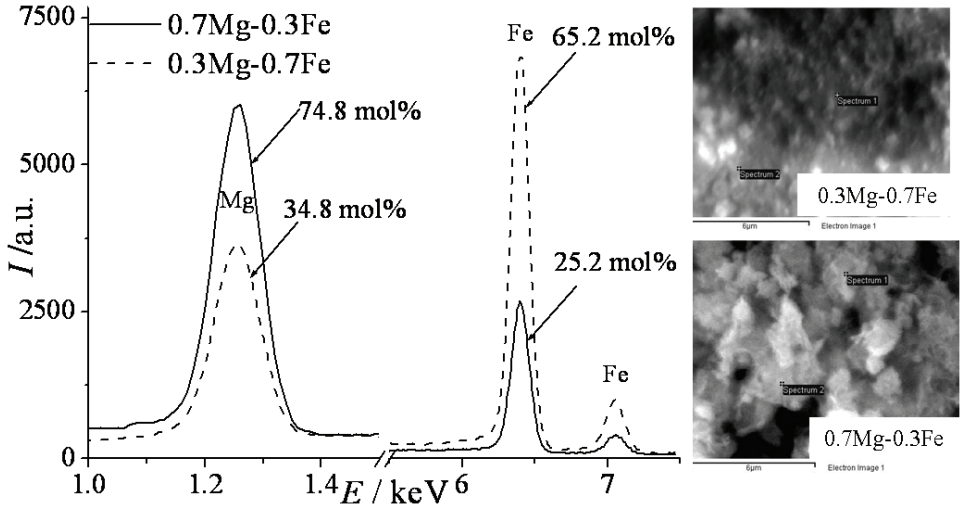

Fig. 2. EDS Analysis of the synthesized samples: 0.3Mg–0.7Fe-LDH and 0.7Mg–0.3Fe-LDH.

The pore size distributions of both calcined samples after the reduction treatment are shown in Fig. 3. It can be observed that after reduction the pore size distribution in both samples had changed. A decrease in a fraction of smaller mesopores and a shift toward higher values for both peak maximum (≈40 nm) and

"shoulder" (60 nm) was observed for the K-0.7Mg–0.3Fe sample, which explains the decrease in surface area (105 m^2 g^{-1}). In the K-0.3Mg–0.7Fe sample, a slight shift in the peak maximum towards mesopores of ≈50 nm diameter and the formation of a small fraction of mesopores with diameter of 3 and 5 nm were detected. The decrease and increase in the mentioned diameter values resulted in an insignificant change in the surface area, from 50 before to 48 m^2 g^{-1} after the reduction.[10] According to the literature, this behavior is explained by the collapse of smaller mesopores in the mixed oxides during the reduction treatment and the formation of mesopores of larger diameters.[4]

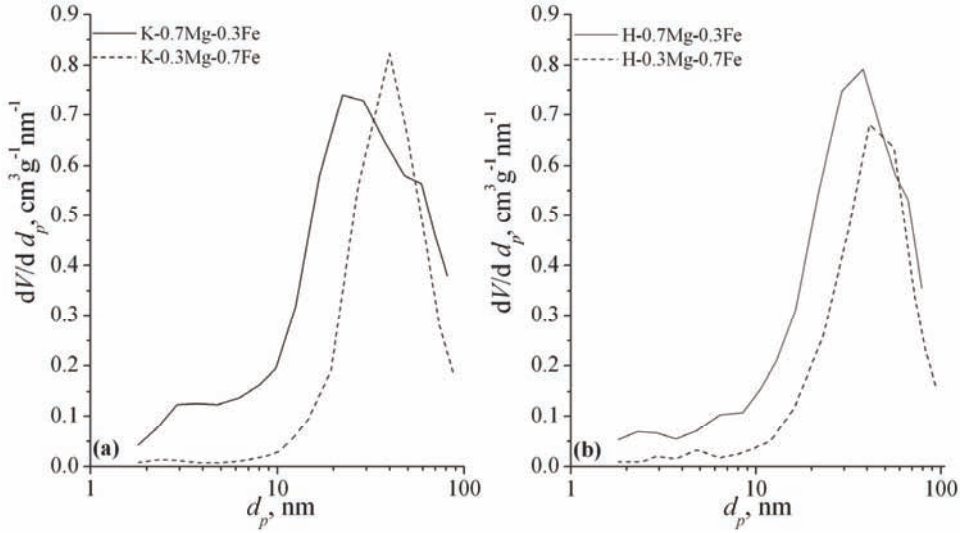

Fig. 3. Pore size distribution of the sample a) after calcination (K-0.7Mg–0.3Fe and K-0.3Mg–0.7Fe) and b) after reduction treatment (H-0.7Mg–0.3Fe and H-0.3Mg–0.7Fe).

The FTIR spectra of the calcined samples and the FTIR spectra of samples after pyridine/phenol adsorption at room temperature in air are presented in Figs. 4 and 5, respectively. Based on the spectra of calcined samples, it can be concluded that all key absorption bands (3455, 2924, 1642 and 1465 cm^{-1}) of the mixed oxides derived from LDH are present with sufficient intensities.[14–16]

The FTIR spectra of the pyridine pre-adsorbed samples are presented in Fig. 5a, in which absorption bands at around 1440 and 1460 cm^{-1} are observed. According to the literature, if an absorption band around 1540 cm^{-1} is detected, this is indicative for pyridinium ions adsorbed on Brønsted acid sites, while bands that appear around 1440 and 1460 cm^{-1} are attributed to coordinatively adsorbed pyridine molecule on Lewis acid sites.[9,17] Therefore, the detected surface acid sites are assigned as Lewis acid sites in both samples. That more intense bands are visible in the spectrum of the K-0.7Mg–0.3Fe-P sample implies a higher num-

ber of acid sites with stronger surface interaction are present on the surface of this sample. The smaller number of acid sites present on the surface of the sample synthesized outside the optimal range for a single phase LDH could be explained by the negative effect of the formation of the additional Fe-phase and smaller fraction of LDH-derived mixed oxide phase.

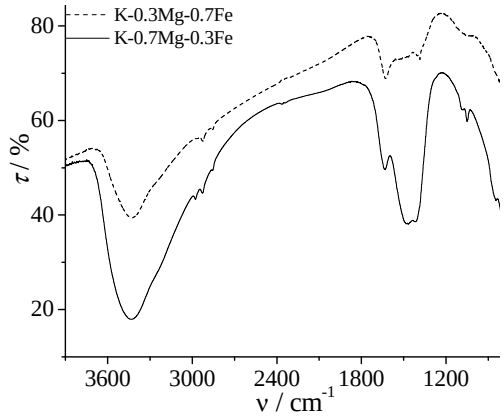

Fig. 4. FTIR Absorption bands of the calcined samples (K-0.7Mg–0.3Fe and K--0.3Mg–0.7Fe).

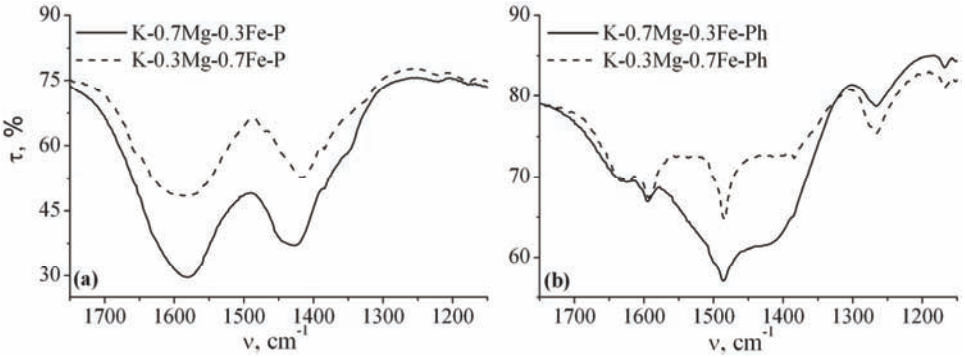

Fig. 5. FTIR Spectra of the calcined samples a) pyridine adsorbed (K-0.7Mg–0.3Fe-P and K-0.3Mg–0.7Fe-P) and b) phenol adsorbed (K-0.7Mg–0.3Fe-Ph and K-0.3Mg–0.7Fe-Ph).

The FTIR analysis of the pre-adsorbed phenol samples (Fig. 5b) showed the presence of absorption bands at around 1604, 1485, 1265 and 1170 cm^{-1} in both samples, assigned to base active sites.[18] According to the literature reference, phenol molecules chemisorbed on base active sites on sample surfaces generate the most intense FTIR absorption bands of their functional groups at wave numbers intervals ranging from 1605–1594, 1485–1475, 1260–1224 and 1180–1170 cm^{-1}. In the spectrum of the sample K-0.7Mg–0.3Fe-Ph with a higher Mg content, more intense peaks related to the adsorbed phenol were detected, indicating a larger number of base active sites on its surface compared to the K-0.3Mg–––0.7Fe-Ph sample. This significant decrease in the number of base active sites on

the K-0.3Mg–0.7Fe-Ph sample surface could be explained by the smaller amount of Mg, the additional Fe-phase and smaller fraction of the LDH-derived mixed oxide phase.

These results support the hypothesis that the FT selectivity should be higher on the K-0.7Mg–0.3Fe-Ph sample due to the higher content of base active sites and the ability of the Mg oxide phase to enhance the selectivity towards FT products of iron catalysts.[4]

The selectivity of all samples at different reaction temperatures (350, 375 and 400 °C) with an H_2:CO ratio of 1:1 are presented in Fig. 6. The sample with the highest Mg content (0.7Mg–0.3Fe), having a larger number of base sites compared to the other sample (0.3Mg–0.7Fe) exhibited lower selectivity at all three reaction temperatures. Comparing the selectivity of samples towards C_4- and C_5-compounds after 100 min of the FT reaction, the sample 0.7Mg–0.3Fe showed low selectivity towards C_4-compounds, while selectivity towards C_5-compounds was not detected despite the variation of the reaction temperature. This low selectivity could be explained by its stable structure, disabling high catalytic performance, observed and published elsewhere.[10] The sample synthesized outside the optimal range and with the highest Fe content showed selectivity towards both C_4- and C_5-compounds after 100 min of FT reaction at all reaction temperatures. Therefore, although the K-0.7Mg–0.3Fe sample, synthesized within the optimal range for single phase LDH, has a larger number of base active sites on the surface, the K-0.3Mg–0.7Fe sample showed higher selectivity, Fig. 6, at all three FT reaction temperatures, implying that other surface properties also have a great impact on catalytic selectivity in the chosen reaction.

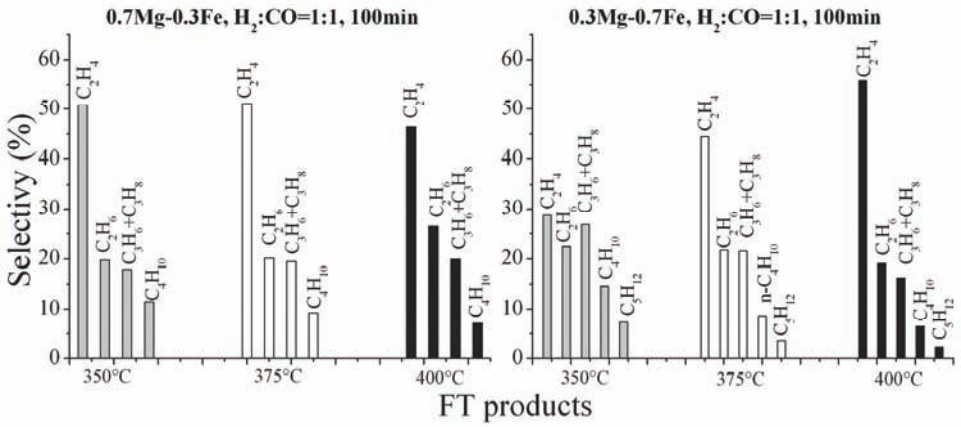

Fig. 6. Selectivity of calcined samples after the reduction process at different FT reaction temperatures after 100 min of the reaction.

The results of textural analysis of both reduced samples before and after the FT reactions at different temperatures are presented in Figs. 7 and 8. The surface area of the reduced H-0.7Mg–0.3Fe sample had not changed significantly after the FT reaction at 350 °C, being also the temperature for the reduction treatment. With increasing FT reaction temperature, the surface area increased, as well as the amount of both larger mesopores (30–40 nm) and the amount of smaller mesopores (2–3 nm), Fig. 8a. This could be explained by the "prolonged" calcinations, evolution of the remaining, trapped carbonates and by the influence of the formed FT products. The increase in surface area, together with better acid––base properties, did not have positive effects on the selectivity in the FT reaction.

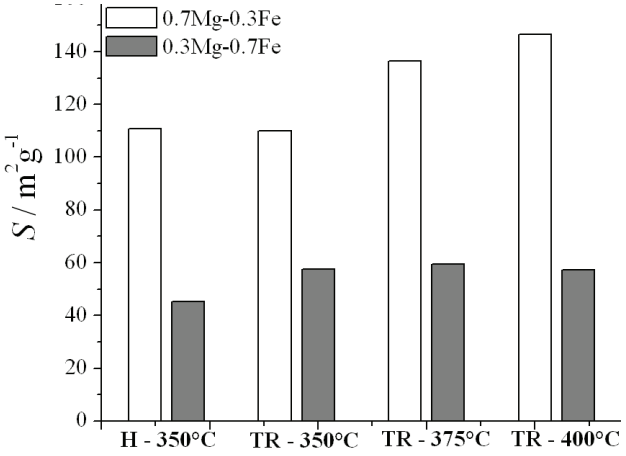

Fig. 7. Surface areas of the reduced, calcined samples before (H – 350 °C) and after FT reactions at different temperatures (TR – 350 °C, TR – 375 °C, TR – 400 °C).

In the sample 0.3Mg–0.7Fe, the surface area slightly increased during the FT reaction, but did not change significantly with change in the reaction temperature, although a small change in the pore size distribution was observed. With increasing reaction temperature, the fraction of larger mesopores in range from 35 to 45 nm decreased with the simultaneous increase in fraction of smaller mesopores in range from 2 to 4 nm (Fig. 8b), resulting in no significant change in the values of surface area (Fig. 7). It should be noted that TG/DTA analysis revealed that the formation of the spinel phase commenced at lower temperatures (≈550 °C) in the sample 0.3Mg–0.7Fe, indicating a less stable structure compared to the 0.7Mg–0.3Fe sample (≈650 °C). Although having a smaller surface area and smaller number of acid–base sites, the 0.3Mg–0.7Fe sample showed higher selectivity towards the desired products in the FT reaction. This is probably due to its metastable structure of a non-stoichiometric mixed oxide, which has a greater influence on the formation of active sites on the catalyst surface than the other investigated surface properties.

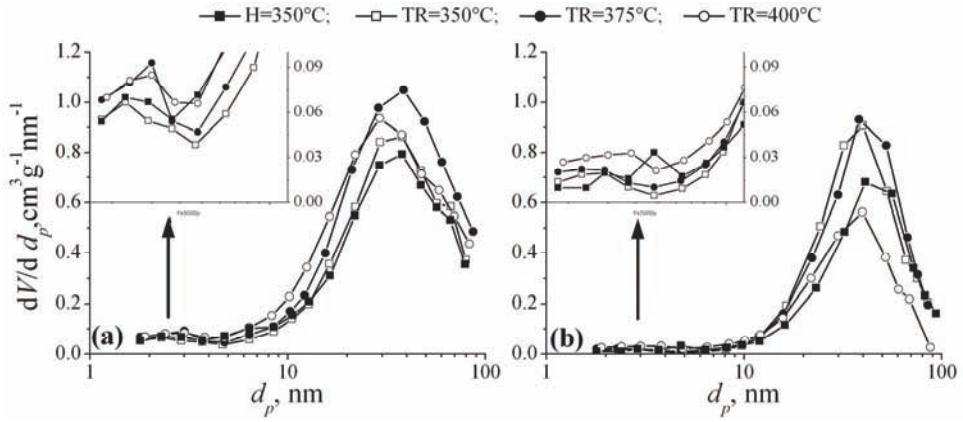

Fig 8. Pore size distribution of samples a) 0.7Mg–0.3Fe and b) 0.3Mg–0.7Fe after the reduction treatment and after FT reactions at different temperatures.

CONCLUSIONS

The characterization of the Mg–Fe-LDH samples confirmed their successful synthesis having an Mg–Fe content in good agreement with desired Mg/Fe ratio set before the synthesis. The properties of the mixed oxides obtained by thermal treatment and their surface properties were highly influenced by the Mg/Fe ratio. Thermal analysis of the synthesized LDHs revealed the formation of more stable mixed oxides when originating from the single LDH phase sample compared to the sample synthesized outside the optimal range. The metastable multiphase system (LDH and additional Fe-phase) with a lower number of surface acid and base active sites, a lower surface area and a smaller fraction of the smaller mesopores showed a higher selectivity in the FT reaction, implying that the metastability of the derived multiphase oxides structure had a greater influence on the formation of active sites on the catalyst surface than the other investigated surface properties.

Acknowledgment. The financial support received from the Ministry of Education and Science of the Republic of Serbia (Contract No. III 45008) is gratefully acknowledged.

И З В О Д

Mg–Fe МЕШОВИТИ ОКСИДИ ДОБИЈЕНИ РАЗГРАДЊОМ ДВОСТРУКИХ СЛОЈЕВИТИХ ХИДРОКСИДА: ИСПИТИВАЊА СВОЈСТАВА ПОВРШИНЕ

МИЛИЦА С. ХАДНАЂЕВ-КОСТИЋ[1], ТАТЈАНА Ј. ВУЛИЋ[1], РАДМИЛА П. МАРИНКОВИЋ-НЕДУЧИН[1], АЛЕКСАНДАР Д. НИКОЛИЋ[2] и БРАНИСЛАВ ЈОВИЋ[2]

[1]Технолошки факултет, Универзитет у Новом Саду, Бул. цара Лазара 1, 21000 Нови Сад и [2]Природно-математички Факултет, Универзитет у Новом Саду

Утицај својстава површине на селективност синтетисаних катализатора је испитиван узимајући у обзир да је селективност према одређеним угљоводоницима од пресудног значаја за укупну активност у одабраној Фишер–Тропш реакцији. Анализирани су двостуки слојевити

хидроксиди са магнезијумом и гвожђем, опште формуле $[Mg_{1-x}Fe_x(OH)_2](CO_3)_{x/2}\cdot mH_2O$, x = = n(Fe)/(n(Mg)+n(Fe)) синтетисани при различитим Mg/Fe односима, као и мешовити оксиди настали њиховом термичком разградњом. Избор градивних метала за синтезу катализатора заснован је на познатим својствима гвожђа, као што су висока активност у Фишер–Тропш реакцији са редокс карактеристикама, као и могућност формирања специфичних активних центара у слојевитој структури LDH; магнезијум је првенствено одабран услед базних својстава одговарајућег оксида. Термички мање стабилан вишефазни систем (синтетисан ван опсега оптималног за синтезу једнофазних LDH са додатном фазом гвожђа) показује већу селективност у Фишер–Тропш реакцији, и поред евидентно мање киселих и базних центара на површини и слабије развијене специфичне површине, уз смањен удео мањих мезопора. Резултати истраживања указују да метастабилност структуре добијених вишефазних оксида има већи утицај на формирање специфичних површинских центара катализатора него остала испитивана својства површине.

(Примљено 29. априла, ревидирано 1. јуна 2011)

REFERENCES

1. K. Kumabe, T. Sato, K. Matsumoto, Y. Ishida, T. Hasegawa, *Fuel* **89** (2010) 2088
2. H. Xiong, M. Moyo, M. A. M. Motchelaho, L. L. Jewell, N. J. Coville, *Appl. Catal., A* **388** (2010) 168
3. N. Lohitharn, J. G. Goodwin, *J. Catal.* **260** (2008) 7
4. J. Yang, Y. Sun, Y. Tang, Y. Liu, *J. Mol. Catal., A* **245** (2006) 26
5. F. Cavani, F. Trifiro, A. Vaccari, *Catal. Today* **11** (1991) 173
6. A. Vaccari, *Catal. Today* **41** (1998) 53
7. V. R. L. Constantino, T. J. Pinnaviaia, *Inorg. Chem.* **34** (1995) 883
8. M. Hadnadjev, T. Vulic, R. Marinkovic-Neducin, Y. Suchorski, H. Weiss, *Appl. Surf. Sci.* **254** (2008) 4297
9. J. A. Lercher, C. Grundling, G. Eder-Mirth, *Catal. Today* **27** (1996) 353
10. M. Hadnađev-Kostić, T. Vulić, R. Marinković-Nedučin, *J. Serb. Chem. Soc.* **75** (2010) 1
11. X. Lei, F. Zhang, L. Yang, X. Guo, Y. Tian, S. Fu, F. Li, D. Evans, X. Duan, *AlChE J.* **53** (2007) 932
12. Z. Yang, K. Choi, N. Jiang, S. Park, *Bull. Korean Chem. Soc.* **28** (2007) 11
13. W. Yanga, Y. Kima, P. Liub, M. Sahimia, T. Tsotsisa, *Chem. Eng. Sci.* **57** (2002) 2945
14. J. Pérez-Ramırez, G. Mul, F. Kapteijn, J. A. Moulijn, *Appl. Catal., A* **204** (2000) 265
15. D. Carriazo, C. Martin, V. Rives, *Eur. J. Inorg. Chem.* (2006) 4608
16. J. T. Kloprogge, R. L. Frost, *J. Solid State Chem.* **146** (1999) 506
17. F. Prinetto, Z. Li, E. Kemnitz, A. Trunschke, J. Deutsch, H. Lieake, A. Auroux, *J. Catal.* **234** (2005) 119
18. I. Poljanšek, M. Krajnc, *Acta Chim. Slovenica* **52** (2005) 238.